Biomedical Signal Processing and Control 101 (2025) 107133

Contents lists available at ScienceDirect

Biomedical Signal Processing and Control

journal homepage: www.elsevier.com/locate/bspc

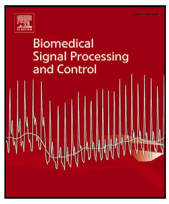

Online automatic detection of phrenic nerve activation during cryoablation procedure for atrial fibrillation treatment

Antonio Gil-Izquierdo [a], Roberto Mateos-Gaitán [a], Francisco M. Melgarejo-Meseguer [b,*], F. Javier Gimeno-Blanes [c], Dafne Lozano-Paredes [b], Juan José Sánchez-Muñoz [a], Arcadi García-Alberola [a], José Luis Rojo-Álvarez [b]

[a] Hospital Clínico Universitario Virgen de la Arrixaca, Ctra. Madrid-Cartagena, s/n, El Palmar, 30120, Murcia, Spain
[b] Universidad Rey Juan Carlos, Cam. del Molino, 5, Fuenlabrada, 28942, Madrid, Spain
[c] Universidad Miguel Hernández de Elche, Av. de la Universitat d'Elx, Elche, 03202, Alicante, Spain

ARTICLE INFO

Keywords:
Phrenic nerve
Signal processing
Atrial fibrillation
Real-time design
Support vector classifier

ABSTRACT

Background and Aim: Cryoballoon ablation is an effective technique for treating Atrial Fibrillation (AF). Its application in the pulmonary vein antrum poses a potential risk of phrenic nerve damage due to its anatomic proximity. Manual protocols are implemented during the ablation procedure to mitigate this risk, although these may be susceptible to subjectivity and variations. In this work, we propose an online system capable of automatically detecting the phrenic nerve integrity during the cryoablation procedure for AF in the pulmonary veins. The system performs digital processing of the ECG signals recorded during the ablation process, detects and segments the ECG signals, and uses a machine learning classifier to infer the risk of damage.
Methods: The used dataset consisted of monitoring system signals obtained from the cryoablation procedures of ten AF patients from Virgen de la Arrixaca University Clinical Hospital in Murcia, Spain. The first stage involves signal processing of the ECG leads, using noise filtering and delineation to unmask any residual cellular potential during phrenic nerve stimulation. A comparative analysis was conducted where the electrocatheter was placed near the phrenic nerve to stimulate it and when the electrocatheter was intentionally displaced, resulting in the phrenic nerve not being stimulated despite an electrical pulse being applied. The detection stage used a linear support vector classifier for both scenarios.
Results: It was possible to automatically classify the level of muscle activity from the phrenic nerve with high accuracy in this known-solution dataset. An online system was created capable of performing and synchronizing all the described stages to manage the signal extracted from the monitoring system.
Conclusion: The system presented here can be a valuable tool for clinical practice, enabling the identification of specific pacing pulses when phrenic nerve involvement occurs, eventually and probably minimizing the use of manual protocols subject to interpretation biases.

1. Introduction

Cryoablation is a widely used and advanced technique in hospital settings, particularly for treating various cardiac arrhythmias, with atrial fibrillation (AF) being its most prevalent target [1]. This minimally invasive therapeutic procedure involves applying frigid temperatures precisely to heart tissue, either to modify the arrhythmia substrates or to disrupt interfering electrical signals that trigger them. Its efficacy lies in its ability to destroy cardiac cells, offering advantages such as improved application stability due to cryoadhesion and the possibility for tissue recovery at lower temperatures [2]. Despite its effectiveness, cryoablation has inherent risks, such as damage to nearby structures in the treatment area, and a usual example is the injury of the phrenic nerve, which can occur during the cryoballoon ablation of pulmonary veins for AF treatment [3]. The phrenic nerve is crucial to the respiratory system, as it innervates the diaphragm and is the essential muscle for breathing [4]. Given its proximity to regions targeted during cryoablation procedures, particularly the pulmonary vein antrum, there is a potential risk of phrenic nerve injury. Damage to the phrenic nerve can result in transient or permanent dysfunction of the ipsilateral diaphragm, subsequently resulting in respiratory challenges for the patient [5]. Clinical studies indicate that transient

* Corresponding author.
E-mail address: francisco.melgarejo@urjc.es (F.M. Melgarejo-Meseguer).

https://doi.org/10.1016/j.bspc.2024.107133
Received 21 May 2024; Received in revised form 9 October 2024; Accepted 2 November 2024
Available online 23 November 2024

diaphragmatic paralysis occurs in approximately 6% of procedures and permanent paralysis in about 0.5% of procedures [6,7]. Given this close connection between the cryoablation procedure and the phrenic nerve, we need to employ precise automatic techniques and patient-specific monitoring to minimize the risk of unintentional damage to nearby structures.

In modern clinical practice, manual safety protocols have been implemented during cardiac ablation procedures to detect any potential phrenic nerve impairment [8]. These techniques involve fluoroscopic monitoring of diaphragmatic excursion or direct manual assessment of diaphragmatic contractions during spontaneous or regular phrenic nerve stimulation. Proper diaphragmatic contraction serves as an indicator of the integrity of the ipsilateral phrenic nerve [9,10]. However, conventional methods are essentially subjective, so there is a need to develop automated and objective methodologies for real-time evaluation of the phrenic nerve during cardiac ablation procedures. For instance, a promising protocol has been described in previous research [11], which is based on methodologies from neurology for evaluating the phrenic nerve through registration and analysis of compound diaphragmatic muscle potentials. The phrenic nerve is electrically stimulated with an electrocatheter, and electrodes placed on the skin detect the muscle action potential. The potential is monitored through the procedure, and a decrease in signal amplitude indirectly indicates damage to the phrenic nerve, resulting in reduced activation of the diaphragmatic muscle. However, the signal monitoring is not automated, and its interpretation remains subjective due to frequent artifacts or signal variations and differences in interpretation among observers. Therefore, developing a tool that enables objective tracking and interpretation of muscle action potential for clinical practice is essential.

For its development, we designed our work in consecutive stages. Advanced signal processing techniques were applied in the first stage, including preprocessing, noise filtering, and delineation. Specifically, we focused on detecting residual cellular muscle potentials during the phrenic nerve stimulation, comparing situations where the sensor is placed directly on the phrenic-nerve muscle (captured activation) with situations where the sensor is intentionally displaced from the phrenic nerve and any muscle (non-captured activation). To detect activity from the phrenic nerve, we proposed to use a Support Vector Machine (SVM) linear classifier to recognize the signals as captured or non-captured. The final stage involved implementing an online system capable of executing the entire methodology in real-time. Using standard signals, this system analyzes the muscular activity in response to phrenic nerve stimulation during the procedure. The present work demonstrates that the proposed system is a valid tool to enhance the safety protocol established during the inpatient ablation procedure [12], adding an automated, unbiased, objective, and online methodology to detect possible unwanted effects that could occur on the phrenic nerve.

This document is structured into four sections. The first section describes several clinical and medical aspects of cryoablation, including its potential effects on the phrenic nerve and the respiratory system. Additionally, it provides an exhaustive review of the scientific literature regarding the procedures performed and the implemented safety techniques. The second section details the methods and methodologies implemented in the proposed solution. The third section presents the different experiments, analyses, and results obtained. Finally, the conclusions and discussion section examines the results concerning the objectives pursued and the improvements achieved.

2. Background

In this section, several relevant aspects related to the existing literature on cryoablation procedures for the suppression of AF and those associated with the phrenic nerve and possible complications during these processes are gathered. This section is divided into several subsections. The first subsection, which focuses on clinical content, summarizes the mechanisms and underlying causes of AF and provides an overview of cryoablation as a therapeutic tool used in these cases. The second subsection covers the complications in the phrenic nerve during these procedures. Additionally, a scientific literature review is included on various existing techniques related to the automated assessment of possible damage.

2.1. Pulmonary vein cryoablation procedure in AF

AF is a widespread cardiac arrhythmia that can negatively impact cardiovascular health. Characterized by irregular and often rapid heartbeats, AF disrupts the regular rhythm of atrial contractions, compromising the heart ability to pump blood effectively [13]. This common condition affects millions worldwide, with a prevalence of 37.574 million cases (0.51% of the global population) in 2020 [14]. Its implications extend beyond irregular heart rhythms, increasing the risk of severe complications, such as stroke, heart failure, and various other cardiovascular issues [15].

Percutaneous catheter ablation is the most effective treatment for restoring sinus rhythm in patients with AF. Numerous studies have shown that the electrical isolation of pulmonary veins through ablating their antrum is the most effective method to prevent AF recurrences, offering a higher success rate and a lower complication rate. This intervention is necessary because it can enhance the quality of life for AF patients by reducing symptoms and decreasing the need for rhythm control medications, which are known for their frequent adverse effects. Additionally, catheter ablation and the restoration of sinus rhythm have demonstrated a positive impact on survival in specific subgroups of AF patients. The most recognized clinical practice guidelines from the European and American Heart Association recommend catheter ablation as a first-line treatment [15].

Cryoablation and radiofrequency ablation are the leading technologies used for ablation procedures. Specifically, for AF, a catheter balloon has been designed to be percutaneously inserted through the femoral vein into the left atrium of the heart and then applied consecutively to the four pulmonary veins antra. Here, a controlled application of freezing temperatures destroys heart cells in direct contact. This technology offers several advantages over radiofrequency, including shorter procedure times while maintaining the same safety and effectiveness [16].

2.2. Phrenic nerve involvement during the procedure

The phrenic nerve plays a crucial role in the respiratory system. It originates from the cervical spine, specifically from the third to the fifth vertebrae (C3 to C5). This nerve significantly impacts the diaphragm, the primary muscle responsible for breathing mechanics. The phrenic nerve acts as a central conduit for neural communication between the brain and the diaphragm, coordinating the intricate sequence of muscle contractions and relaxations necessary for inhalation and exhalation [4]. This neural communication is essential for the rhythmic process of breathing. Serving as a vital conduit [17], the nerve relays neural commands that regulate the contraction and relaxation of the diaphragm.

This anatomical connection gains heightened importance in the context of AF cryoablation. During this cardiac procedure, the proximity of the phrenic nerve becomes a critical consideration. In humans, the distance between the phrenic nerve and the right superior pulmonary vein is approximately 2–3 mm [18]. Therefore, during the ablation of pulmonary veins, there is a risk of damaging the phrenic nerve, leading to diaphragmatic paresis, resulting in discomfort and difficulty breathing [5]. While the phrenic nerve can be injured in various arrhythmia ablation procedures, the most common occurrence is during cryoballoon ablation for AF. Long-term phrenic nerve damage is risky even when cooling to −35 °C.

It is essential to have a thorough knowledge of phrenic nerve anatomy, recognize specific stages in the ablation process that pose a higher risk of nerve damage, and be familiar with existing techniques to prevent such complications. Furthermore, in instances where this complication does occur, swift recognition of its presence is crucial. Understanding the natural progression and potential recovery of nerve function at early stages or higher temperatures allows for timely monitoring of phrenic nerve damage. Prompt recognition enables the procedure to cease and avoid further phrenic nerve injury.

2.3. Phrenic nerve injury prevention in literature

This section examines scientific research on the automated assessment of phrenic nerve injury prevention, focusing on its applicability to evaluating the phrenic nerve during ablation. Through a comprehensive synthesis of existing literature, this part aims to explain the rapid advancements in techniques for assessing phrenic nerve integrity during ablation procedures.

The most straightforward and commonly employed techniques to avoid phrenic nerve injury during various arrhythmia ablations are based on pacemapping. Intuitively, the ability to stimulate the phrenic nerve (indicated by a distinctive jerky diaphragmatic contraction, known as a *capture*) from an endocardial site allows the operator to identify areas close to the nerve. This indicates that ablation should be avoided in these areas due to the risk of nerve injury. Additionally, over the last decades, technological developments have enabled recording these points in virtual 3D heart maps made during the procedure, enhancing the safety of procedures and allowing precise localization of the nerve path.

However, during the cryoballoon ablation procedure, pacemapping is not usually performed due to technical limitations with the catheter, higher costs, complications, and increased procedure time, which add complexity to an already intricate procedure. In this scenario, the surveillance of phrenic nerve integrity is typically performed by manually monitoring diaphragmatic function under regular phrenic nerve stimulation. The operator can recognize a reduction or lack of diaphragmatic contraction during spontaneous breathing or phrenic nerve stimulation by placing a hand over the thorax or using a fluoroscopic view. If this occurs, phrenic nerve affectation is assumed, and the application is immediately stopped. However, variations in catheter or hand position, excessively low pacing outputs, and breathing oscillations can misguide the operator, deciding to continue or halt subjective. Moreover, this approach does not prevent phrenic nerve injury. Instead, it allows the application to be stopped early, making a transient lesion more likely than a permanent one.

The electromyogram (EMG) of the diaphragm has been used to assess phrenic nerve integrity to improve monitoring and attempt to predict nerve lesions before they appear. Several results in muscle monitoring, developed in electromyography and neurophysiology, proposed the use of compound muscle action potential (CMAP) to monitor phrenic nerve behavior [19,20]. These authors based their work on the insights demonstrated in [21], which recorded the electrical response of the diaphragm when it is stimulated by an electrical stimulus applied through the skin with a needle electrode or by an endovascular catheter placed near the phrenic nerve.

A more straightforward method involved using superficial electrodes placed on the skin, specifically modified leads or standard leads used in cardiology during procedures or for a standard electrocardiogram (ECG). The ECG recorded had two distinct components: one from the pacing artifact and the other from the supposed electrical activity of the diaphragm. A reduction of more than 30% in the signal amplitude of this second component can predict a phrenic nerve lesion and subsequent diaphragmatic paralysis. Although evidence was limited, this methodology was tested in preclinical and clinical studies during cryoballoon ablation procedures, demonstrating acceptable reliability and reducing the incidence of phrenic nerve lesions [20]. These results have been applied by other researchers who tried to find less invasive methods to monitor the CMAP based on modified versions of lead I, [22–29], all of them finding close results. CMAP monitoring is better when performed by a catheter placed near the hepatic vein, but it is difficult to perform and requires another catheter during the procedure. They also reported that using a modified version of lead I is useful in detecting phrenic nerve injury. Still, it presents several problems, such as other electrical signals or environmental factors that can influence muscle activity ECG, varying pacing stimulus intensities, signal filtering, or respiratory cycles, all of which reduce reliability [11]. On the other hand, [30] proposed a score map of the CMAP for early detection of phrenic nerve damage during ablation. This score map was created using template matching and a 3-dimensional electroanatomic mapping system. They reported that this score map can detect drops in CMAP due to phrenic nerve injury faster than CMAP monitoring.

As we can observe, the timing from the first reduced amplitude of the ECG signal to halting the ablation is crucial. All of these methods require a second operator who manually conducts this monitoring during the procedure, which can lead to frequent inaccuracies or delayed detection, thereby limiting the effectiveness of the technique. In this context, we developed an automatic system capable of enabling real-time analysis and objective interpretation of the CMAP of the diaphragm. This tool will offer an effective and reliable way to monitor phrenic nerve integrity.

3. Methods

This section explains our methodology for evaluating phrenic nerve muscle activity and its detection. The technical part of our work can be divided into three stages. The first stage involves extracting signals from raw files obtained from the monitoring system and applying preprocessing, filtering, and delineation techniques to isolate and detect the electrical stimulation generated by the phrenic nerve. In the second stage, we use a linear classifier based on SVM to differentiate between regular nerve activity and affected activity. The third stage involves implementing a system to execute all this processing and a machine-learning detector in real-time, yielding visual information about the different stimuli and a final decision flag, indicating if there could be damage risk from the observed phrenic nerve activity.

3.1. Signal processing scheme

This first stage establishes a comprehensive protocol for monitoring phrenic nerve stimuli in patients undergoing AF treatment via cryoablation. This protocol involves extracting ECG signals from the monitoring system and applying advanced signal processing techniques to delineate and isolate stimuli responses within the ECG signal, both on and off the phrenic nerve. The goal is to create a consistent dataset to develop the experiment.

A multi-phase approach is implemented to achieve accurate detection and isolation of stimuli. The methodology encompasses three phases, namely preprocessing, delineation, and template characterization. The preprocessing phase employs high-pass filters with a specific cutoff frequency of 100 Hz to identify and separate the sharp peaks indicative of stimuli in the ECG signal [31]. This filter effectively suppresses low-frequency components, focusing the analysis on the relevant high-frequency signal content. Subsequent correlation techniques are applied to map these identified peaks back to the original ECG signal while ensuring information integrity. Delineation is further refined by trend removal, allowing for signal segmentation [31]. Following this segmentation, stimulation templates are generated by aggregating individual signals acquired through windowing and applying a specially developed event detector. This process produces standardized stimulation templates, thus simplifying the subsequent automatic classification phase for each case and lead.

As previously described, given the nature of the stimulus response, high-pass filtering is employed to isolate the stimuli from the rest of the cardiac signal. Continuing with this filtered signal, we apply a peak detector based on the maximum detection technique. These detected peaks are retrieved from the original signal to avoid losing information about the stimuli. Next, a template stimulus is created based on the different stimuli within the selected window. To achieve this, we use the detected peaks in the original signal as our reference to isolate the various stimuli. The template beat is created from this series of stimuli, which is the median of all these windows we have generated.

After acquiring stimulation templates for each lead and scenario outlined earlier, we conducted a comprehensive mathematical characterization to complete this phase. This involved assessing the amplitudes, durations, and time-offsets of these templates based on clinical criteria [9]. Comparative analysis of muscle activity across the various evaluated scenarios was performed to discern the effective activation of the phrenic nerve, focusing on distinguishing differences between captured and non-captured instances.

3.2. Machine learning scheme

The following phase focuses on categorizing and characterizing two primary states, namely, the presence and absence of muscular activity in response to the phrenic nerve. To achieve this, we employed a linear SVM classifier, which is a machine-learning algorithm capable of establishing linear decision boundaries for data classification. This classifier aids in distinguishing and categorizing these distinct states based on the acquired data. The SVM algorithm aims to draw optimal linear decision boundaries between different data classes. It focuses on finding an optimal hyperplane that maximizes class separation in a multi-dimensional space. This hyperplane is determined to best separate data points, maximizing the distance between them and the nearest points of each class. This approach facilitates the classification of new data points based on their position relative to the hyperplane, facilitating precise separation of different classes of linearly separable data in a higher-dimensional space [32].

The optimal hyperplane, responsible for separating data points of distinct classes, is fine-tuned to achieve adequate segregation. Linear classifiers offer benefits such as computational efficiency and scalability for large datasets. Their clear delineation through linear functions also establishes decision boundaries, making them easy to interpret. This transparency aids in clarifying the relationship between input features and class labels, emphasizing their interdependence. To illustrate this approach, consider a labeled dataset:

$$\mathbf{X} \in \mathbb{R}^{L \times N} \text{ and } \mathbf{y} \in \mathbb{R}^{L} \tag{1}$$

where $\mathbf{X}$ is the data matrix consisting of L samples of patients arranged in rows, denoted by $\mathbf{x}_i$ for $i = 1, .., L$, and N different characteristics in columns. A binary output variable $\mathbf{y} \in \mathbb{R}^{L}$ is also available, defined as a vector of classes or labels, such that $y_i \in \{-1, +1\}$ for $i = 1, .., L$. The optimal plane that separates the two classes is defined as:

$$f(\mathbf{x}) = \mathbf{w}\mathbf{x}^T + b = 0, \tag{2}$$

where $\mathbf{x}$ is the input vector, $\mathbf{w}$ is the weight vector and b is the bias. The following inequalities are fulfilled:

$$\mathbf{w}\mathbf{x}_i^T + b \geq +1 \text{ if } y_i = 1, \quad \mathbf{w}\mathbf{x}_i^T + b \leq -1 \text{ if } y_i = -1. \tag{3}$$

The SVM objective function aims to find the new $\mathbf{w}$ and b so that the hyperplane effectively separates the data and maximizes the margin $1/\|\mathbf{w}\|^2$. Vectors $\mathbf{x}_i$ for which $|y_i|\left(\mathbf{w}\mathbf{x}_i^T + b\right) = 1$ are denominated support vectors. They can also be within the margin or considering the opposite class (−1). Establishing the optimal hyperplane involves identifying these support vectors, which are crucial data points closest to the decision boundary. They significantly influence the orientation and placement of the hyperplane, enhancing the linear classifier ability to make accurate predictions [33]. The careful selection and positioning of these support vectors are pivotal in capturing essential characteristics and patterns necessary for precise classification. Therefore, this algorithm is appropriate for distinguishing between two categories and identifying instances of either correct phrenic nerve activity or reduced activity, potentially indicating nerve impairment.

3.3. Online detection scheme

We propose designing and implementing an online system capable of executing the different processing and machine-learning phases in real-time, thereby completing the developed protocol. As shown in Fig. 1 this setup is structured into four stages, each crucial for integrating clinical signal extraction, advanced processing techniques, machine learning, and visualization of results.

In the clinical extraction phase during the ablation procedure, immediately following the emission of a square pulse from the stimulator, we capture real-time signals from the twelve ECG leads recorded by the monitoring system. These signals encompass the entire ECG waveform, including the response to the pulse across all twelve leads. Subsequently, the signal undergoes rigorous preprocessing in the stimulation detector phase. Key to this phase is the application of advanced filtration techniques to enhance signal delineation. Specifically, a high-pass filter with a cutoff frequency of 100 Hz is employed to isolate sharp peaks indicative of stimuli in the ECG signal. Following filtration, correlation techniques are utilized to accurately map these identified peaks back to the original ECG signal to preserve information.

The next stage consists of template characterization in which the signal is further defined by trend removal, allowing for precise signal segmentation. Following this identification, a machine learning stage emerges based on the stimulation templates generated by aggregating individual signals acquired through windowing. Once stimulus templates from the twelve leads are obtained, they are adapted into our pre-trained SVM model for instantaneous decision-making. The extracted real-time ECG signals and the corresponding stimulus templates are visualized on a monitor to provide clear insights. We utilize a traffic light design with three distinct states to represent the final decision. The first state is grey, indicating no stimulation, and the protocol is inactive. The second state is red, represented by the top LED, signaling the non-capture of phrenic nerve activity despite stimulation, which could indicate a procedure-related issue. The final state is green, represented by the lower LED, signifying the successful capture of phrenic nerve activity following stimulation, thus confirming its proper functioning. This approach provides a universal language [34]: Green signifies the procedure is functioning correctly, red indicates the need to stop the protocol, and grey shows that the protocol is inactive. This clear and intuitive design enhances the usability and effectiveness of the monitoring system in clinical settings.

4. Dataset and experiments

This section presents the dataset, experiments, and results obtained, structured into four subsections. The first subsection describes the dataset used. The second subsection introduces signal preprocessing, including isolating and detecting the impulse caused by the stimulus. The third subsection describes the experiments conducted with SVM classifiers to classify stimulus-induced muscle activity. Finally, the fourth subsection presents the various visualizations of the developed online tool, enabling the clinical team to monitor both the real-time signals and the alerts generated by the classifier.

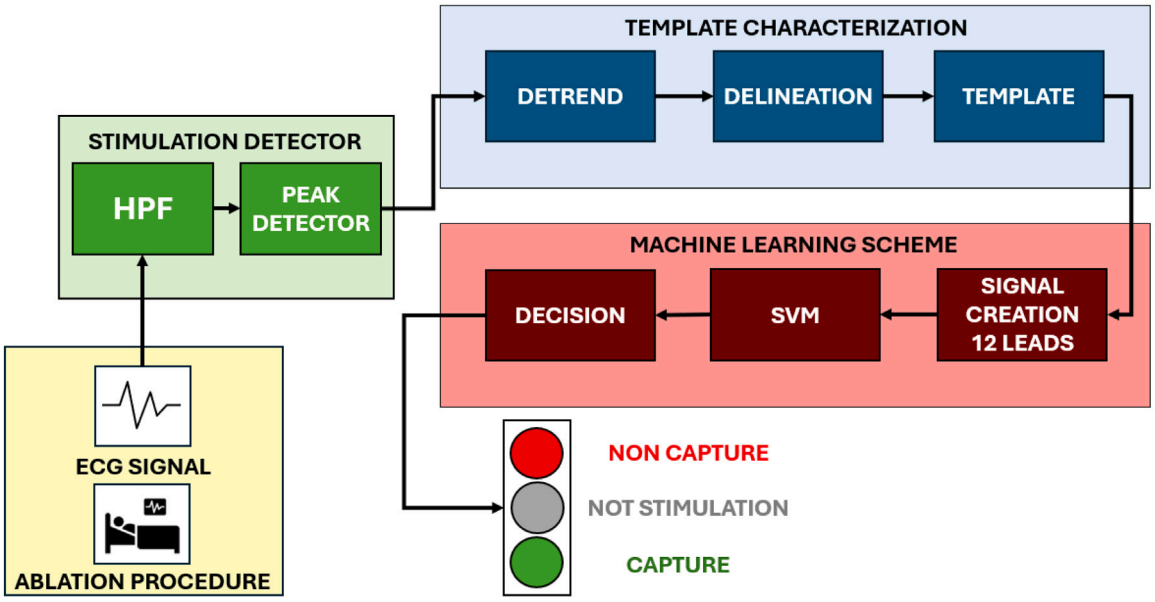

Fig. 1. Online scheme scenario representing the complete process.

4.1. Patients and dataset

The stimulation strategy used on the phrenic nerve consists of two stages. In the first stage, a series of stimulations are performed directly on the phrenic nerve using the intracavitary catheter. In the second stage, air stimulation is conducted, where the intracavitary catheter is used without contacting any tissue that could provoke a response from the phrenic nerve. The response to these impulses is studied directly on the surface ECG of the monitoring system connected to the patient. The stimulation protocol consists of trains of four to six periodic stimuli with a static amplitude, separated by one to two seconds, depending on the characteristics of the patient. These stimuli are programmed with different amplitude and frequency configurations. The four cases studied are ×2 and ×4 in amplitude and 50 and 250 Hz in frequency to assess the response to the different stimuli.

This study selected ten cases recorded during ablation procedures for AF at the Virgen de la Arrixaca University Clinical Hospital in Murcia. The signals were recorded using a monitoring system with ECG electrodes placed in standard positions on the patient's skin. As previously mentioned, some of the registered leads can capture the compound muscle action potential of the diaphragm. Following established clinical protocols, these electrodes are essential during a standard cryoablation procedure for heart rhythm monitoring.

The dataset used in this study consists of 10 cases with the following demographics: three women and seven men, aged between 55 and 72, with an average age of 66,5 years. This sample represents a diverse range in terms of gender and age according to the identified pathology. These demographic characteristics reflect an older adult population undergoing the cryoablation procedure to treat AF. This dataset provides a solid basis for analyzing and assessing phrenic nerve muscle activity during the procedure.

We address two distinct scenarios to comprehensively analyze phrenic nerve muscle activity. In the first scenario, referred to as *capture*, an electrocatheter is percutaneously inserted through a femoral vein puncture and positioned near the right phrenic nerve in the distal superior vena cava to pace it regularly. With proper stimulation (commonly a square electric pulse of 2 ms and 5–20 milliamps), the phrenic nerve is activated regularly (*captured*), and the diaphragmatic muscle responds with an immediate contraction (*hiccup*), recognized by manual monitoring by the operator with a hand over the thorax. If this occurs during the ablation, it indirectly represents the preserved integrity of the ipsilateral phrenic nerve. If diaphragmatic contractions stop, it indicates a lack of integrity of the phrenic nerve. In the second scenario, an electrocatheter is placed intentionally in areas unrelated to the phrenic nerve to administer and register the same electrical artifact but without capturing the phrenic nerve and with the subsequent absence of compound muscle potential, confirmed manually by the lack of diaphragmatic contraction. This protocol was repeated with different low-pass signal filtering at 50 and 100 Hz, respectively. This approach provides a crucial comparative perspective when assessing how the presence or absence of compound muscle potential influences the registered ECG, as observed in Fig. 2.a, and how signal filtering modifies or alters the signal, offering a more comprehensive understanding of the system reliability.

4.2. Results on signal processing

Firstly, to study the behavior of the stimulus generated for analysis, we utilize the ECG leads from the monitoring system signals, observing a square pulse of variable duration. In Fig. 2.b, we present an example of a real pulse of this type. The response to the impulse suggests the appearance of the stimulus in the surface ECG with two consecutive peaks. The Synchronization of the first peak with the stimulation signal observed in Fig. 3 and its linearity in response to the square pulse amplitude led us to define it as an artifact. Conversely, the second peak's non-linearity of the response to the impulse in the stimulus, along with its stable morphology in response to frequency changes, led us to consider that this peak corresponded to the muscular activity of the phrenic nerve, as defined in several previous studies [9,11].

To confirm this, we conducted a series of measurements of amplitudes and differences between peaks for all patients and cases. These measurements are summarized in Table 1, which compiles the amplitude difference between the first and second peaks across all standard ECG leads. Upon reviewing the results, we observed similar variations in amplitude for both peaks when capturing nerve activity, confirming the presence of phrenic nerve muscle activity in both instances. Conversely, in cases of non-capture, we observed that the second peak consistently remained present, indicating persistent artifact even if a significant portion appeared in the first peak. Based on this consistent behavior across all leads, we analyze the entire stimulus,

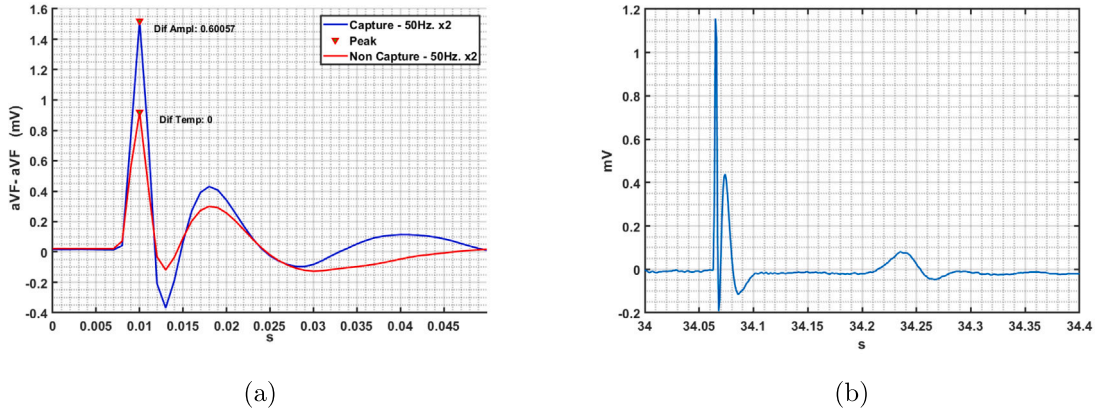

Fig. 2. Illustrations of stimuli in varied contexts: (a) Contrasting stimuli shape in capture and non-capture scenarios. (b) Depicting the form of phrenic stimulation in aVF Lead.

Table 1
Results for the time-windowing experiment.

Lead	Difference (Absolute)	Difference (Relative)
I	1.44 ± 2.20	26.85% ± 92.53%
II	2.11 ± 1.36	49.07% ± 26.85%
III	0.39 ± 0.57	4.28% ± 40.30%
aVR	1.90 ± 1.77	24.71% ± 95.56%
aVL	0.01 ± 1.67	−126.84% ± 160.46%
aVF	**1.37 ± 0.75**	**41.46% ± 19.65%**
V1	0.41 ± 0.57	22.00% ± 26.03%
V2	1.12 ± 1.11	38.81% ± 25.89%
V3	1.08 ± 1.02	35.55% ± 36.05%
V4	1.17 ± 1.01	44.02% ± 26.57%
V5	1.23 ± 0.98	49.20% ± 23.07%
V6	1.20 ± 0.78	48.27% ± 24.34%

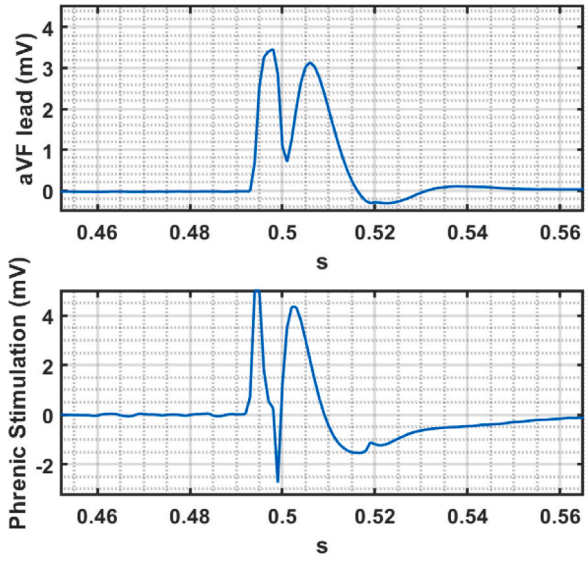

Fig. 3. Synchronization between stimulation and response in ECG leads.

including measurements of amplitude, areas, and differences. Once our experimental strategy was established, we analyzed 60 pre-existing subsamples to prepare the data for our linear classifier.

4.3. Results on machine learning

Once the data was classified, we utilized our linear classifier to distinguish between signals *with capture* and those *without capture*. This approach helped us identify instances of phrenic nerve muscle activity

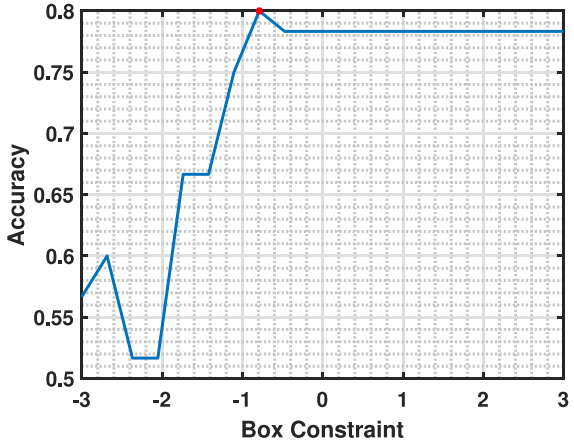

Fig. 4. Average accuracy in hyperparameter searching procedure from linear SVM.

versus those absent, providing insight into the adequacy of catheter placement or potential nerve affectation. We could differentiate between these two classes using the SVM, enabling us to assess and quantify the nerve activity.

To achieve robust results with the classifier, we collectively analyzed all twelve leads for each case. This method provides comprehensive insights into the stimulus within the ECG signal. Given the limited number of cases available, we employed one case for training and nine for testing in our classifier configuration. The hyperparameter selection was performed by applying a 10-fold cross-validation technique in which the optimized parameter is the SVM-box constraint (related to the C parameter). It was inspected across a uniform grid ranging from 10^{-3} to 10^{3}, achieving an accuracy ratio of 0.8 with a box constraint of about 0.063, as it can be seen in 4.

Following this experiment, we achieved a result of 100% accuracy in detecting phrenic nerve muscle activity within this moderate dataset [12]. This underscores the efficacy of our methodology and encourages its implementation in a natural environment.

The main weakness of this method is the lack of cases we have access to. For this reason, we conducted a bootstrap analysis. The results are illustrated in Fig. 6. Note that feature relevance was computed by selecting those features for which the 95% confidence interval of their weight, after the bootstrap procedure, does not overlap zero. These are represented in blue in the figure. Features that overlap zero are represented in red. Furthermore, to ensure the generalizability of this model, we evaluated the accuracy achieved during this bootstrap procedure, as depicted in Fig. 7. As can be observed, the accuracy of the proposed method is 70% or higher in more than 90% of the examples, yielding 76.05% ± 12.77% of mean and standard deviation.

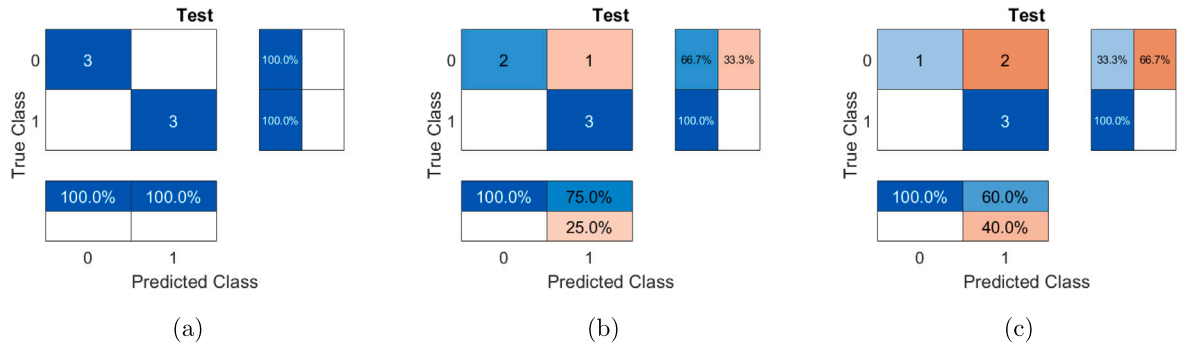

Fig. 5. SVM confusion matrix for different window sizes, showing the results for: (a) A 5-s window; (b) A 3-s window; And (c) a 1-s window. In all subpanels, 0 stands for non-capture, and 1 stands for capture.

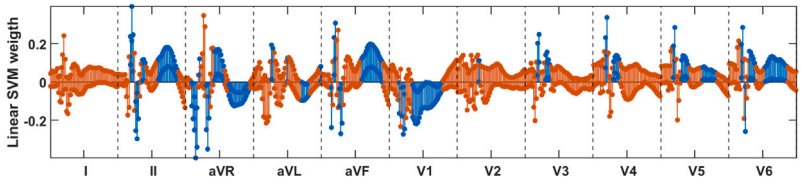

Fig. 6. Linear SVM weight computed with the bootstrap procedure. Blue lines report the valid features, while red ones represent those where the confidence interval at 95% overlaps zero.

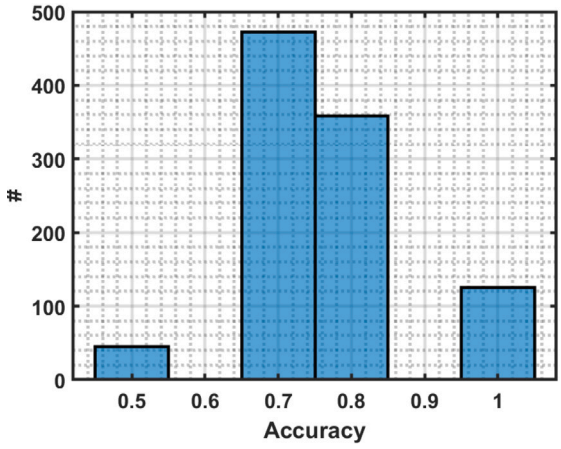

Fig. 7. Histogram of accuracy achieved during 1000 samples bootstrap procedure.

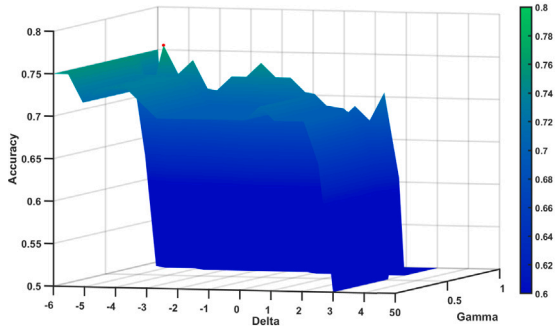

Fig. 8. Average accuracy in hyperparameter searching procedure from LDA.

The model generalization to other centers should not present significant issues because the cryoablation protocol is highly standardized across different institutions. Phrenic nerve stimulation is performed in all centers using the same types of catheters and from the same anatomical locations. ECG recording protocols are also standardized, including filters, leads, cutaneous electrodes, sampling frequency, and amplification. All commercial electrophysiology polygraphs used in hospitals record ECG with similar quality.

Regarding plans for validation on a broader population, the next step would be to demonstrate that the system can detect phrenic nerve injury earlier (or at least not later) than conventional methods such as mechanical palpation or fluoroscopic control. The challenge lies in phrenic nerve injury occurring in only a small percentage of patients, and a study would require a very large sample size to draw solid conclusions. Ideally, the algorithm would be incorporated into a commercial polygraph or cryoablation system, automatically allowing its use in dozens or hundreds of centers, enabling large-scale validation.

To put the features of our proposal in context, we compared the performance of the linear SVM with another well-known linear classifier, the linear discriminant analysis (LDA). For this comparison, we performed the same hyperparameter search procedure. However, in this case, the limits for the parameters delta and gamma were $[10^{-6}, 10^{3}]$ and $[0, 1]$, respectively. These results are depicted in Fig. 8, where it can be observed that the accuracy achieved is lower than that achieved by the SVM method. We also computed the classification weights of our trained LDA, which are presented in Fig. 9. Both weight profiles are different when comparing Figs. 9 and 6. Noticeably, both methods identify certain parts as relevant, specifically, the first part of aVR and the last part of II, aVL, aVF, V1, V2, V4, and V5. These parts appear to be important in both methods. This can be explained by the fact that these signal segments change the most when detecting affection of the phrenic nerve.

4.4. Results with online detector

One of the experiments we implemented involved reducing the decision-making window to expedite the process. We tested three different intervals: the original five-second interval, a three-second interval, and a final one-second interval. Our observations indicated that as the window duration increased, accuracy improved, rising from 66.3% to 100% for the five-second window, as shown in Fig. 5. The intermediate three-second window resulted in an accuracy of 83.3

To verify the accuracy of our methodology, we examined the weights of the linear classifier for the test across the three experiments,

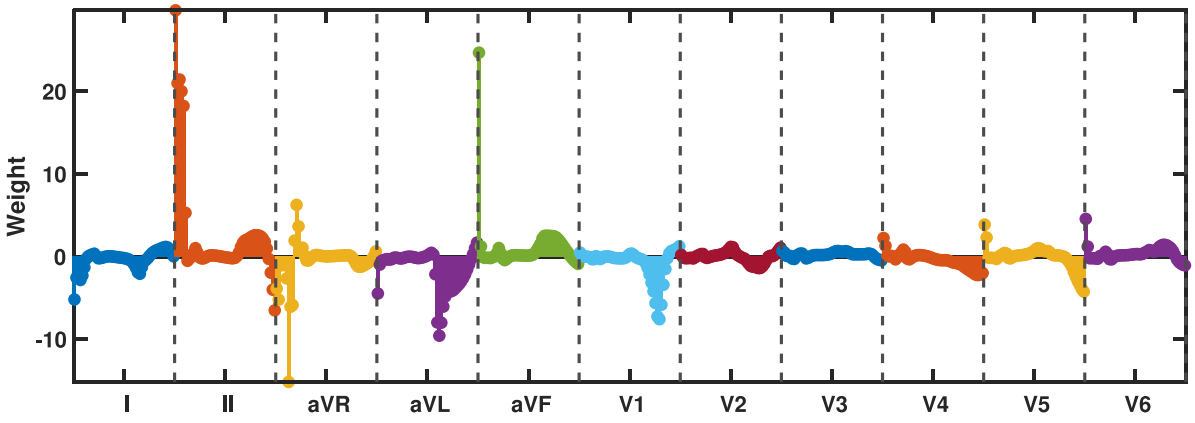

Fig. 9. LDA classification weights.

Table 2
Results for time windowing experiment.

Windows (s)	Time (s)	Rise time (s/w)	Rise time (%)	Accuracy (%)
5	64	5.33	106	100
3	123	6.15	205	83.3
1	283	4.72	472	66.7

as shown in Fig. 10. The five-second clearly emphasized both signal peaks, while the shorter window resulted in a deformed shape. However, due to the variability in the impulse response and the arbitrariness in stimulation (a stimulus generated within the ECG signal will be added), we decided to discard the one-second option, opting to consider only the three-second and five-second windows.

Once we obtained the results from the linear classifier and a wide selection of signals lasting over a minute, we were ready to implement an online system capable of detecting phrenic nerve muscle activity in real-time. To achieve this objective, we utilized the configurable parameter of the analysis window, which determines the number of seconds analyzed to make a decision.

We conducted a timing evaluation experiment to determine the optimal windowing configuration by applying the entire process in real-time. For this purpose, we calculated the response time per window to assess the viability of the procedure as a complete package. We used a system with basic specifications, including an Intel i7 processor, an NVIDIA GTX 1050ti graphics card, and 16 GB of RAM. This choice ensured the scalability of the process for implementation on any computer in an Electrophysiology Laboratory.

The results presented in Table 2 indicate that the optimization reaches its maximum efficiency with a five-second window, achieving a relative response time of 106%. In comparison, the three-second window has a response time double that of the five-second window, registering 205%. Notably, the one-second window, which was previously discarded, shows even more unfavorable performance, with a response time of 472%, approximately five times higher than the five-second window. Based on clinical experience and these results, where stimulation occurs roughly every second and a half, we have set a window duration of five seconds to obtain consistent stimulus templates. This allows us to determine whether the muscle activity is being captured every five seconds of the signal.

To achieve a representation suitable for the clinical environment of an operating room, we considered creating two simultaneous figures. The upper figure will display a real-time representation of the original signal. In contrast, the lower figure will depict the templates obtained for each interval to verify the proper functioning and evolution of the stimulus over time. Additionally, to represent the decision, we designed a traffic light with three lights: red indicates that the phrenic nerve muscle activity is not being captured, green signals indicate normal capture is occurring, and gray indicates that the phrenic nerve is not being stimulated. This state is updated at each working interval. As shown in Fig. 11, we ran the method for three real cases of one-minute duration in our optimal five-second windowing. In case (a), we show a case of damage to the phrenic nerve, producing a negative trend in the amplitude of the stimulus. We observe how the template decreases amplitude until the method detects the damage. A final green capture template also corresponds to an adjustment in the catheter positioning. For the second case (b), a displacement in the catheter causes the alarm state to be generated. We observe that the amplitude is not changing, but a displacement in the catheter is causing a lack of phrenic nerve activity. Finally, in (c), we observe another case of phrenic nerve damage in which the negative trend in the stimulus occurs again, and the damage is detected from the third window.

During the experimentation phase, we encountered difficulty among some clinicians in distinguishing between the green and red signals at the traffic light due to deuteranomaly [35]. We implemented a consistent solution to address this without deviating from the universal representation system. Instead of changing the color coding, we introduced a two-second tone whenever the phrenic nerve signal was not captured. This addition indicates an anomalous case, suggesting the possibility that the phrenic nerve may be affected in such situations. Furthermore, to maintain a historical record of the progression during stimulation protocols, we store a signal composed of a colored-coded language in which 0 stands for *no capture*, 1 signifies *no stimulation*, and 2 denotes *capture*. This signal is synchronized with the monitoring system time, enabling access to the results post-procedure.

Therefore, after reviewing the implemented setup, we can conclude that we have designed a real-time online system capable of receiving signals from the twelve leads and making decisions regarding the existence of phrenic nerve muscle activity within a five-second working window, achieving a 100% accuracy in our moderate dataset.

5. Discussion and conclusion

Cryoablation has demonstrated efficacy in treating cardiac arrhythmias, notably with cryoballoon ablation of the pulmonary vein antrum in AF. However, its proximity to the phrenic nerve presents inherent risks of injury. This nerve is crucial for diaphragm control and breathing, necessitating careful consideration during ablation. Traditional manual safety protocols that mitigate risks are susceptible to subjectivity and procedural variations. In this context, our work introduces an objective machine learning online system designed to detect real-time diaphragmatic muscle activation and indirectly assess phrenic nerve integrity during AF cryoablation, aiming to enhance clinical assessment and streamline intervention strategies.

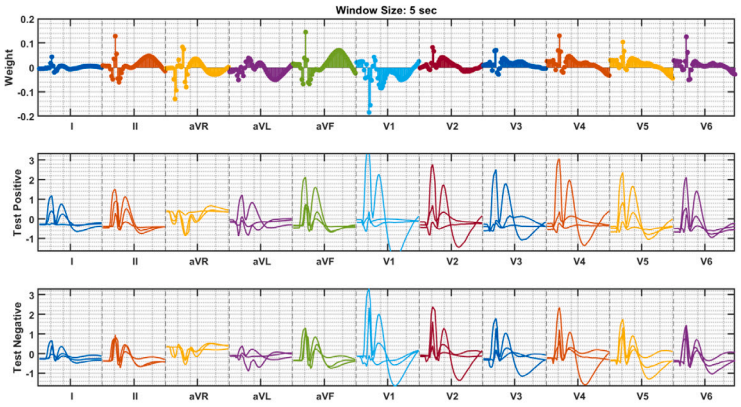

(a)

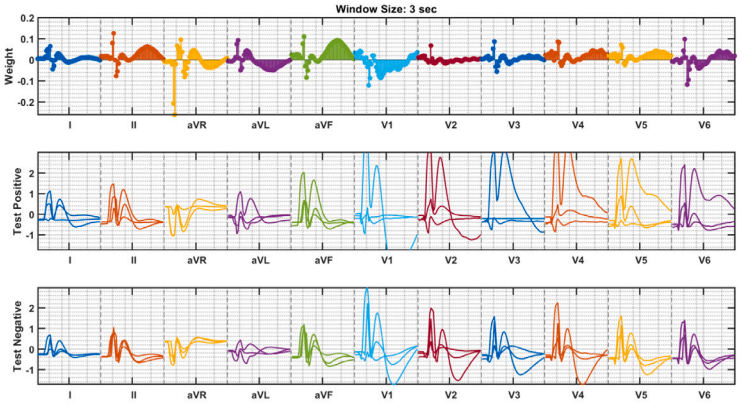

(b)

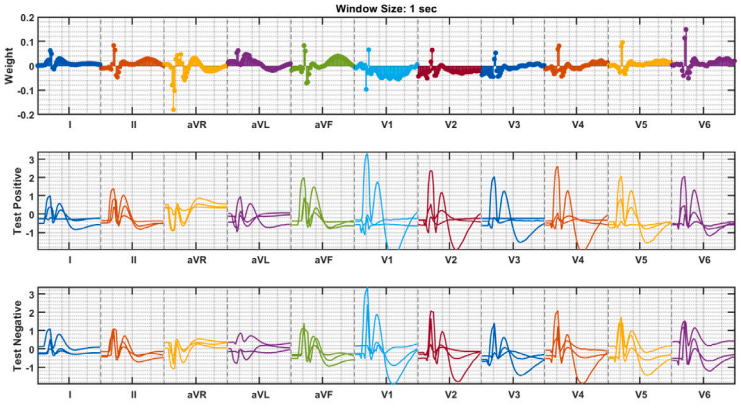

(c)

Fig. 10. SVM performance for different window sizes. Results are depicted for a 5-s window (a), for a 3-s window (b), and for a 1-s window (c). Each panel is divided into three sub-panels, representing the linear SVM weight for each input sample, an example of a signal classified as capture, and an example classified as non-capture.

Our methodology unfolds in three stages: signal processing, machine learning, and online system deployment. We utilized ten monitoring system signals obtained from ablation procedures performed at Virgen de la Arrixaca University Clinical Hospital. Our primary focus was implementing advanced signal processing techniques, including preprocessing, noise filtering, and delineation. Specifically, we aimed to reveal cellular muscle potential residues during phrenic nerve stimulation. Through a meticulous comparative analysis between direct electrocatheter placement near the phrenic nerve (capture) and intentional displacement (no capture), our linear classifier adeptly characterizes muscle activity associated with phrenic nerve activation.

Results from the linear SVM classifier indicate high accuracy in automatically classifying real-time monitoring system signals within this dataset, confirming the system's capability to accurately assess phrenic nerve muscle activity levels. This study did not utilize more complex

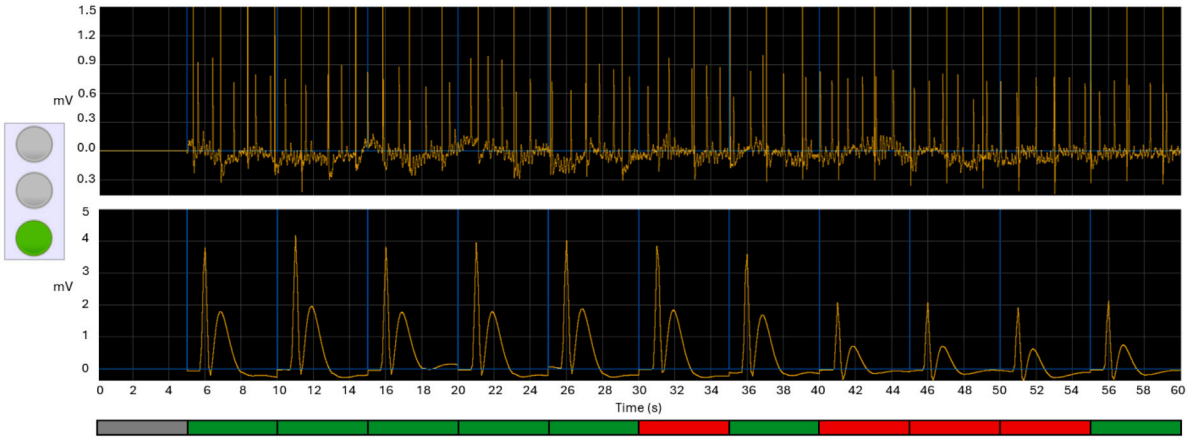

(a)

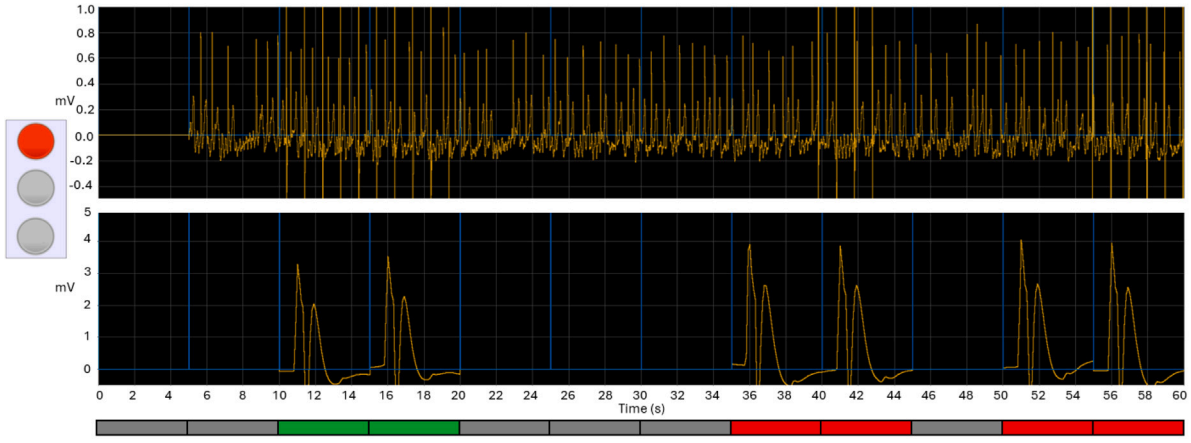

(b)

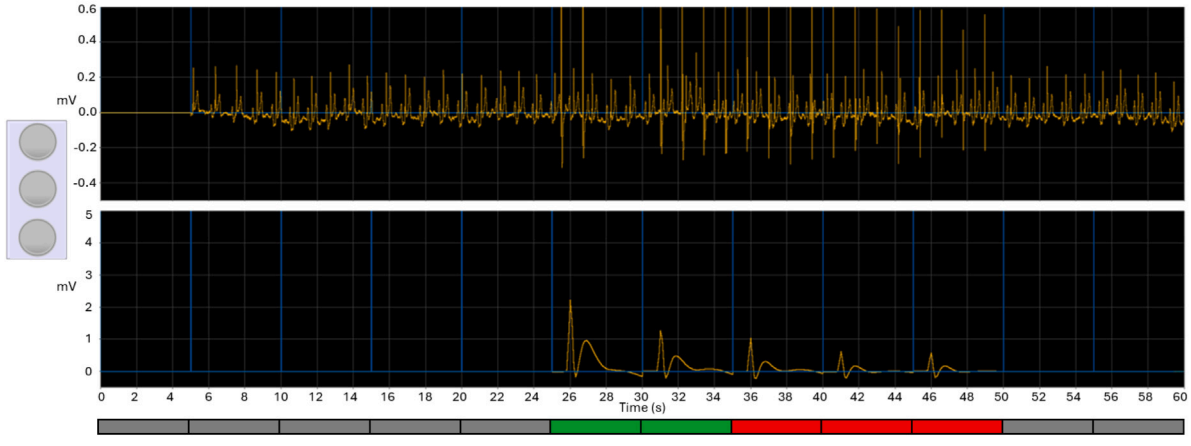

(c)

Fig. 11. Online detection for three real cases applying our methodology.

classifiers, such as deep convolutional neural networks (CNNs). Previous works, such as [36,37], demonstrate the potential of CNNs to extract key features from images and perform highly accurate classifications. While these advanced techniques could potentially enhance our system, our current focus was on leveraging the simplicity and interpretability of the linear SVM model for this initial phase of development. Our work demonstrates that more significant coefficients correspond to the ECG leads where phrenic nerve stimulation issues are more observable, which generally aligns with the leads traditionally recognized by clinicians based on their experience. Additionally, SVM coefficients that are rougher (smoother) in a particular lead compared to their neighboring time coefficients are associated with local variance (averaging) characteristics. The developed online system seamlessly integrates all stages, providing synchronized management of extracted monitoring system signals in real time. A five-second window is necessary to achieve complete accuracy, resulting in a display delay of five seconds. Using such windows reduces the processing frequency, minimizing the need for higher computational capacity. In our case,

the computing time on conventional computers (Intel i7 processor and 16 GB of RAM) can be more than 5.33 s per window. In contrast, with a one-second window with poorer detection performance, the execution times worsen to 4.77 s per window. The integrated monitor displays offer a universal representation of potential issues during cryoablation, specifically concerning phrenic nerve muscular activity.

From a practical application perspective, the ideal user interface for our real-time monitoring system would be integrated into one of the existing systems used for procedural oversight. The most obvious choice is the electrophysiology polygraph, which displays the ECG and other parameters during ablation and is constantly monitored by an experienced operator. An additional window on this system could display phrenic nerve parameters. Another viable option is incorporating the system into the cryoablation console, which also has a control screen. For instance, some well-known manufacturers have a console with a graphical interface to display the phrenic nerve EGM trace during the procedure. Since both the polygraph and the cryoablation console are essential for the procedure, no additional hardware would be needed. Additionally, since both devices are essentially computers, various features could be added, such as graphical or auditory alarms and automated processes to halt the procedure if necessary. Moreover, this integration allows the system to assess the quality of the signal and determine its acceptability before the cryoablation process begins, thus ensuring that the signal quality is adequate for analysis without compromising patient safety. If the signal is weak or noisy, the clinicians are informed, enabling them to make informed decisions on how to proceed.

Integrating our system into these existing platforms would streamline its adoption and minimize disruptions to the clinical workflow. The primary challenge would ensure seamless integration and interoperability with different manufacturers' systems. Moreover, thorough validation and training would be required to ensure clinicians are comfortable and confident in using the new interface. The proposed approach would enhance real-time monitoring capabilities without needing extra equipment, eventually improving patient safety and procedural efficiency.

This is the first algorithm that automatically detects hazardous processes on the phrenic nerve during ablation procedures. The strengths of this method are evident; it provides automatic support to clinicians, surpassing the traditional method, which involves the detection of phrenic nerve affliction via manual detection of spasmodic movements of the diaphragm during the procedure. However, the greatest weakness of our method is the limited number of patients available for validation. We only have data from ten patients, which poses a challenge that needs to be addressed. A method that safeguards against phrenic nerve lesions, which can lead to several respiratory-related issues, must be tested across numerous cases. Nevertheless, this proof of concept paves the way for testing with more patients and developing more secure methods.

CRediT authorship contribution statement

Antonio Gil-Izquierdo: Writing – review & editing, Writing – original draft, Visualization, Software, Methodology, Investigation, Data curation. **Roberto Mateos-Gaitán:** Writing – review & editing, Writing – original draft, Visualization, Methodology, Investigation, Data curation. **Francisco M. Melgarejo-Meseguer:** Writing – review & editing, Writing – original draft, Visualization, Validation, Supervision, Resources, Methodology, Investigation, Formal analysis, Conceptualization. **F. Javier Gimeno-Blanes:** Writing – review & editing, Writing – original draft, Supervision, Software, Project administration, Methodology, Investigation, Formal analysis, Conceptualization. **Dafne Lozano-Paredes:** Writing – review & editing, Writing – original draft, Visualization, Software. **Juan José Sánchez-Muñoz:** Writing – review & editing, Writing – original draft, Validation, Supervision, Investigation, Formal analysis, Data curation, Conceptualization. **Arcadi García-Alberola:** Writing – review & editing, Writing – original draft, Validation, Supervision, Methodology, Investigation, Formal analysis, Data curation, Conceptualization. **José Luis Rojo-Álvarez:** Writing – review & editing, Writing – original draft, Visualization, Validation, Supervision, Resources, Project administration, Methodology, Investigation, Funding acquisition, Formal analysis, Conceptualization.

Declaration of competing interest

The authors declare that they have no known competing financial interests or personal relationships that could have appeared to influence the work reported in this paper.

Acknowledgments

This work was supported by the Research Grants meHeart, HERMES, LATENTIA, and PCardioTrials (PID2019-104356RB-C42, PID2023-152331OA-I00, PID2022-140786NB-C31, and PID2022-140553OA-C42), it was funded by MICIU/AEI/10.13039/501100011033 and ERDF/EU. The work was also partially supported by the HERMES project (2024/00004/006) by Universidad Rey Juan Carlos.

Data availability

Data will be made available on request.

References

[1] J. Chen, R. Lenarczyk, S. Boveda, R. Richard Tilz, A. Hernandez-Madrid, P. Ptaszynski, J. Pudulis, N. Dagres, Cryoablation for treatment of cardiac arrhythmias: results of the European heart rhythm association survey, EP Eur. 19 (2) (2017) 303–307, http://dx.doi.org/10.1093/europace/eux001.

[2] M. Handler, G. Fischer, M. Seger, R. Kienast, F. Hanser, C. Baumgartner, Simulation and evaluation of freeze-thaw cryoablation scenarios for the treatment of cardiac arrhythmias, BioMed. Eng. OnLine 14 (1) (2015) http://dx.doi.org/10.1186/s12938-015-0005-9.

[3] B. Avitall, A. Kalinski, Cryotherapy of cardiac arrhythmia: From basic science to the bedside, Heart Rhythm 12 (10) (2015) 2195–2203, http://dx.doi.org/10.1016/j.hrthm.2015.05.034.

[4] M.A. Greenfield, Phrenic nerve block, in: Pain Management, Elsevier, 2007, pp. 1169–1172, http://dx.doi.org/10.1016/b978-0-7216-0334-6.50144-8.

[5] V.J. Aguirre, P. Sinha, A. Zimmet, G.A. Lee, L. Kwa, F. Rosenfeldt, Phrenic nerve injury during cardiac surgery: Mechanisms, management and prevention, Heart Lung Circ. 22 (11) (2013) 895–902, http://dx.doi.org/10.1016/j.hlc.2013.06.010.

[6] H. Calkins, G. Hindricks, R. Cappato, Y.-H. Kim, E.B. Saad, L. Aguinaga, J.G. Akar, V. Badhwar, J. Brugada, J. Camm, P.-S. Chen, S.-A. Chen, M.K. Chung, J.C. Nielsen, A.B. Curtis, D.W. Davies, J.D. Day, a. d'Avila, N.N. de Groot, L. Di Biase, M. Duytschaever, J.R. Edgerton, K.A. Ellenbogen, P.T. Ellinor, S. Ernst, G. Fenelon, E.P. Gerstenfeld, D.E. Haines, M. Haissaguerre, R.H. Helm, E. Hylek, W.M. Jackman, J. Jalife, J.M. Kalman, J. Kautzner, H. Kottkamp, K.H. Kuck, K. Kumagai, R. Lee, T. Lewalter, B.D. Lindsay, L. Macle, M. Mansour, F.E. Marchlinski, G.F. Michaud, H. Nakagawa, a. Natale, S. Nattel, K. Okumura, D. Packer, E. Pokushalov, M.R. Reynolds, P. Sanders, M. Scanavacca, R. Schilling, C. Tondo, H.-M. Tsao, A. Verma, D.J. Wilber, T. Yamane, 2017 HRS/EHRA/ECAS/APHRS/SOLAECE expert consensus statement on catheter and surgical ablation of atrial fibrillation, Heart Rhythm 14 (10) (2017) e275–e444, http://dx.doi.org/10.1016/j.hrthm.2017.05.012.

[7] J.G. andrade, O.M. Wazni, M. Kuniss, N.M. Hawkins, M.W. Deyell, G.-B. Chierchia, S. Nissen, A. Verma, G.A. Wells, R.D. Turgeon, Cryoballoon ablation as initial treatment for atrial fibrillation, J. Am. Coll. Cardiol. 78 (9) (2021) 914–930, http://dx.doi.org/10.1016/j.jacc.2021.06.038.

[8] M. Lakhani, F. Saiful, V. Parikh, N. Goyal, S. Bekheit, M. Kowalski, Recordings of diaphragmatic electromyograms during cryoballoon ablation for atrial fibrillation accurately predict phrenic nerve injury, Heart Rhythm 11 (3) (2014) 369–374, http://dx.doi.org/10.1016/j.hrthm.2013.11.015.

[9] A. Resman-Găspĕrsč, S. Podnar, Phrenic nerve conduction studies: Technical aspects and normative data, Muscle Nerve 37 (1) (2007) 36–41, http://dx.doi.org/10.1002/mus.20887.

[10] M. Kowalski, K.A. Ellenbogen, J.N. Koneru, Prevention of phrenic nerve injury during interventional electrophysiologic procedures, Heart Rhythm 11 (10) (2014) 1839–1844, http://dx.doi.org/10.1016/j.hrthm.2014.06.019.

[11] P.S. Sharma, S.K. Padala, J.J. Thompson, S. Gunda, J.N. Koneru, K.A. Ellenbogen, Factors influencing diaphragmatic compound motor action potentials during cryoballoon ablation for atrial fibrillation, J. Cardiovasc. Electrophysiol. 27 (2016) 1384–1389, http://dx.doi.org/10.1111/jce.13082.

[12] R. Mateos-Gaitán, A. Gil-Izquierdo, F.-J. Gimeno-Blanes, F.-M. Melgarejo-Meseguer, C. Muñoz-Esparza, J. Luis Rojo-Alvarez, A. García-Alberola, J.-J. Sánchez-Muñoz, Signal processing and machine learning automated evaluation of phrenic nerve affectation by cardiac stimulation, in: Computing in Cardiology Conference (CinC), in: CinC2023, Computing in Cardiology, 2023, http://dx.doi.org/10.22489/cinc.2023.282.

[13] A.J. Wood, E.L. Pritchett, Management of atrial fibrillation, New Engl. J. Med. 326 (19) (1992) 1264–1271, http://dx.doi.org/10.1056/nejm199205073261906.

[14] G. Lippi, F. Sanchis-Gomar, G. Cervellin, Global epidemiology of atrial fibrillation: An increasing epidemic and public health challenge, Int. J. Stroke 16 (2) (2020) 217–221, http://dx.doi.org/10.1177/1747493019897870.

[15] G. Hindricks, T. Potpara, N. Dagres, E. Arbelo, J.J. Bax, C. Blomström-Lundqvist, G. Boriani, M. Castella, G.-a. Dan, P.E. Dilaveris, L. Fauchier, G. Filippatos, J.M. Kalman, M. La Meir, D.A. Lane, J.-P. Lebeau, M. Lettino, G.Y.H. Lip, F.J. Pinto, G.N. Thomas, M. Valgimigli, I.C. Van Gelder, B.P. Van Putte, C.L. Watkins, P. Kirchhof, M. Kühne, V. Aboyans, a. Ahlsson, P. Balsam, J. Bauersachs, S. Benussi, A. Brandes, F. Braunschweig, A.J. Camm, D. Capodanno, B. Casadei, D. Conen, H.J.G.M. Crijns, V. Delgado, D. Dobrev, H. Drexel, L. Eckardt, D. Fitzsimons, T. Folliguet, C.P. Gale, B. Gorenek, K.G. Haeusler, H. Heidbuchel, B. Iung, H.A. Katus, D. Kotecha, U. Landmesser, C. Leclercq, B.S. Lewis, J. Mascherbauer, J.L. Merino, B. Merkely, L. Mont, C. Mueller, K.V. Nagy, J. Oldgren, N. Pavlović, R.F.E. Pedretti, S.E. Petersen, J.P. Piccini, B.A. Popescu, H. Pürerfellner, D.J. Richter, M. Roffi, a. Rubboli, D. Scherr, R.B. Schnabel, I.A. Simpson, E. Shlyakhto, M.F. Sinner, J. Steffel, M. Sousa-Uva, P. Suwalski, M. Svetlosak, R.M. Touyz, N. Dagres, E. Arbelo, J.J. Bax, C. Blomström-Lundqvist, G. Boriani, M. Castella, G.-a. Dan, P.E. Dilaveris, L. Fauchier, G. Filippatos, J.M. Kalman, M. La Meir, D.A. Lane, J.-P. Lebeau, M. Lettino, G.Y.H. Lip, F.J. Pinto, G. Neil Thomas, M. Valgimigli, I.C. Van Gelder, C.L. Watkins, T. Delassi, H.S. Sisakian, D. Scherr, A. Chasnoits, M.D. Pauw, E. Smajić, T. Shalganov, P. Avraamides, J. Kautzner, C. Gerdes, A.A. Alaziz, P. Kampus, P. Raatikainen, S. Boveda, G. Papiashvili, L. Eckardt, V. Vassilikos, Z. Csanádi, D.O. Arnar, J. Galvin, A. Barsheshet, P. Caldarola, A. Rakisheva, I. Bytyçi, A. Kerimkulova, O. Kalejs, M. Njeim, A. Puodziukynas, L. Groben, M.A. Sammut, A. Grosu, A. Boskovic, A. Moustaghfir, N.d. Groot, L. Poposka, O.-G. Anfinsen, P.P. Mitkowski, D.M. Cavaco, C. Siliste, E.N. Mikhaylov, L. Bertelli, D. Kojic, R. Hatala, Z. Fras, F. Arribas, T. Juhlin, C. Sticherling, L. Abid, I. Atar, O. Sychov, M.G.D. Bates, N.U. Zakirov, 2020 ESC guidelines for the diagnosis and management of atrial fibrillation developed in collaboration with the European association for cardio-thoracic surgery (EACTS), Eur. Heart J. 42 (5) (2020) 373–498, http://dx.doi.org/10.1093/eurheartj/ehaa612.

[16] K.-H. Kuck, J. Brugada, A. Fürnkranz, a. Metzner, F. Ouyang, K.J. Chun, A. Elvan, T. Arentz, K. Bestehorn, S.J. Pocock, J.-P. Albenque, C. Tondo, Cryoballoon or radiofrequency ablation for paroxysmal atrial fibrillation, New Engl. J. Med. 374 (23) (2016) 2235–2245, http://dx.doi.org/10.1056/nejmoa1602014.

[17] D.T. Frazier, W.R. Revelette, Role of phrenic nerve afferents in the control of breathing, J. Appl. Physiol. 70 (2) (1991) 491–496, http://dx.doi.org/10.1152/jappl.1991.70.2.491.

[18] D. Sanchez-Quintana, J.A. Cabrera, V. Climent, J. Farré, a. Weiglein, S.Y. Ho, How close are the phrenic nerves to cardiac structures? Implications for cardiac interventionalists, J. Cardiovasc. Electrophysiol. 16 (3) (2005) 309–313, http://dx.doi.org/10.1046/j.1540-8167.2005.40759.x.

[19] P.E. Barkhaus, S.D. Nandedkar, M. de Carvalho, M. Swash, E.V. Stålberg, Revisiting the compound muscle action potential (CMAP), Clin. Neurophysiol. Pract. 9 (2024) 176–200, http://dx.doi.org/10.1016/j.cnp.2024.04.002.

[20] F. Franceschi, M. Dubuc, P.G. Guerra, S. Delisle, P. Romeo, E. Landry, L. Koutbi, L. Rivard, L. Macle, B. Thibault, M. Talajic, D. Roy, P. Khairy, Diaphragmatic electromyography during cryoballoon ablation: a novel concept in the prevention of phrenic nerve palsy, Heart Rhythm 8 (6) (2011) 885–891, http://dx.doi.org/10.1016/j.hrthm.2011.01.031.

[21] O.N. Markand, J.C. Kincaid, R.A. Pourmand, S.S. Moorthy, R.D. King, Y. Mahomed, J.W. Brown, Electrophysiologic evaluation of diaphragm by transcutaneous phrenic nerve stimulation, Neurology 34 (5) (1984) 604, http://dx.doi.org/10.1212/wnl.34.5.604.

[22] B. Mondésert, J.G. andrade, P. Khairy, P.G. Guerra, A. Shohoudi, K. Dyrda, L. Macle, L. Rivard, B. Thibault, M. Talajic, D. Roy, M. Dubuc, Clinical experience with a novel electromyographic approach to preventing phrenic nerve injury during cryoballoon ablation in atrial fibrillation, Circ.: Arrhythm. Electrophysiol. 7 (4) (2014) 605–611, http://dx.doi.org/10.1161/circep.113.001238.

[23] S. Miyazaki, N. Ichihara, H. Taniguchi, H. Hachiya, H. Nakamura, E. Usui, Y. Kanaji, T. Takagi, J. Iwasawa, A. Kuroi, K. Hirao, Y. Iesaka, Evaluation of diaphragmatic electromyograms in radiofrequency ablation of atrial fibrillation: Prospective study comparing different monitoring techniques, J. Cardiovasc. Electrophysiol. 26 (3) (2014) 260–265, http://dx.doi.org/10.1111/jce.12571.

[24] F. Franceschi, L. Koutbi, E. Gitenay, J. Hourdain, B. Maille, L. Trévisan, J.-C. Deharo, Electromyographic monitoring for prevention of phrenic nerve palsy in second-generation cryoballoon procedures, Circ.: Arrhythm. Electrophysiol. 8 (2) (2015) 303–307, http://dx.doi.org/10.1161/circep.115.002734.

[25] T. Deneke, a. Mügge, K. Nentwich, P. Halbfaß, Phrenic nerve injury during isolation of the superior vena cava: Prevention using diaphragmatic compound motor action potentials – "primum nil nocere.", J. Cardiovasc. Electrophysiol. 27 (4) (2016) 396–398, http://dx.doi.org/10.1111/jce.12946.

[26] S. Miyazaki, N. Ichihara, H. Nakamura, H. Taniguchi, H. Hachiya, M. Araki, T. Takagi, J. Iwasawa, A. Kuroi, K. Hirao, Y. Iesaka, Prospective evaluation of electromyography-guided phrenic nerve monitoring during superior vena cava isolation to anticipate phrenic nerve injury, J. Cardiovasc. Electrophysiol. 27 (4) (2016) 390–395, http://dx.doi.org/10.1111/jce.12912.

[27] A. Meissner, P. Maagh, A. Christoph, A. Oernek, G. Plehn, ECG-guided surveillance technique in cryoballoon ablation for paroxysmal and persistent atrial fibrillation: A strategy to prevent from phrenic nerve palsy, Int. J. Med. Sci. 13 (6) (2016) 403–411, http://dx.doi.org/10.7150/ijms.14383.

[28] J.L. Gilge, E.N. Prystowsky, B.J. Padanilam, B.A. Clark, A. Shah, L.A. Steinberg, G.V. Nair, P.J. Patel, Use of diaphragmatic compound motor action potential monitoring to prevent right phrenic nerve palsy during atrial tachycardia ablation, HeartRhythm Case Rep. 7 (11) (2021) 739–742, http://dx.doi.org/10.1016/j.hrcr.2021.08.001.

[29] L. Tovmassian, B. Maille, L. Koutbi, J. Hourdain, E. Martinez, M. Zabern, J.-C. Deharo, F. Franceschi, Diaphragmatic CMAP monitoring during cryoballoon procedures: Surface vs. Hepatic recording comparison and limitations of this approach, Front. Cardiovasc. Med. 9 (2022) http://dx.doi.org/10.3389/fcvm.2022.814026.

[30] A. Mahajan, C. Girman, F.A. Subzposh, P. Vijayaraman, Novel automated "score mapping" of diaphragmatic compound motor action potential for the early detection of phrenic nerve injury during cryoablation, Heart Rhythm 20 (9) (2023) 1339–1340, http://dx.doi.org/10.1016/j.hrthm.2023.06.012.

[31] F.-M. Melgarejo-Meseguer, E. Everss-Villalba, F.-J. Gimeno-Blanes, M. Blanco-Velasco, Z. Molins-Bordallo, J.-A. Flores-Yepes, J.-L. Rojo-Álvarez, A. García-Alberola, On the beat detection performance in long-term ECG monitoring scenarios, Sensors 18 (5) (2018) 1387, http://dx.doi.org/10.3390/s18051387.

[32] D. Mladenić, J. Brank, M. Grobelnik, N. Milic-Frayling, Feature selection using linear classifier weights: interaction with classification models, in: Proceedings of the 27th Annual International ACM SIGIR Conference on Research and Development in Information Retrieval, in: SIGIR04, ACM, 2004, http://dx.doi.org/10.1145/1008992.1009034.

[33] H.-G. Yeom, I.-H. Jang, K.-B. Sim, Variance considered machines: Modification of optimal hyperplanes in support vector machines, in: 2009 IEEE International Symposium on Industrial Electronics, IEEE, 2009, http://dx.doi.org/10.1109/isie.2009.5214295.

[34] R. Morant Marco, Lenguaje semafórico y transformación social, Estudios Lingui Stica Esp. 41 (2020) 43–62.

[35] G.P. Mosquera, M. de Jesús Arteaga Segarra, Alteraciones en la visión cromáticas por agentes neurotóxicos en pacientes de 20 a 40 años, Rev. Vive 4 (2021) 44–52, http://dx.doi.org/10.33996/revistavive.v4i10.74.

[36] I. Iqbal, M. Younus, K. Walayat, M.U. Kakar, J. Ma, Automated multi-class classification of skin lesions through deep convolutional neural network with dermoscopic images, Comput. Med. Imaging Graph. 88 (2021) 101843, http://dx.doi.org/10.1016/j.compmedimag.2020.101843.

[37] I. Iqbal, K. Walayat, M.U. Kakar, J. Ma, Automated identification of human gastrointestinal tract abnormalities based on deep convolutional neural network with endoscopic images, Intell. Syst. Appl. 16 (2022) 200149, http://dx.doi.org/10.1016/j.iswa.2022.200149.